# GSA DATA REPOSITORY 2013259

# Thermal decomposition along natural faults during earthquakes

Cristiano Collettini, Cecilia Viti, Telemaco Tesei, Silvio Mollo

**Data Repository Item DR1**: Structural details of the Principal Slip Zone (PSZ)

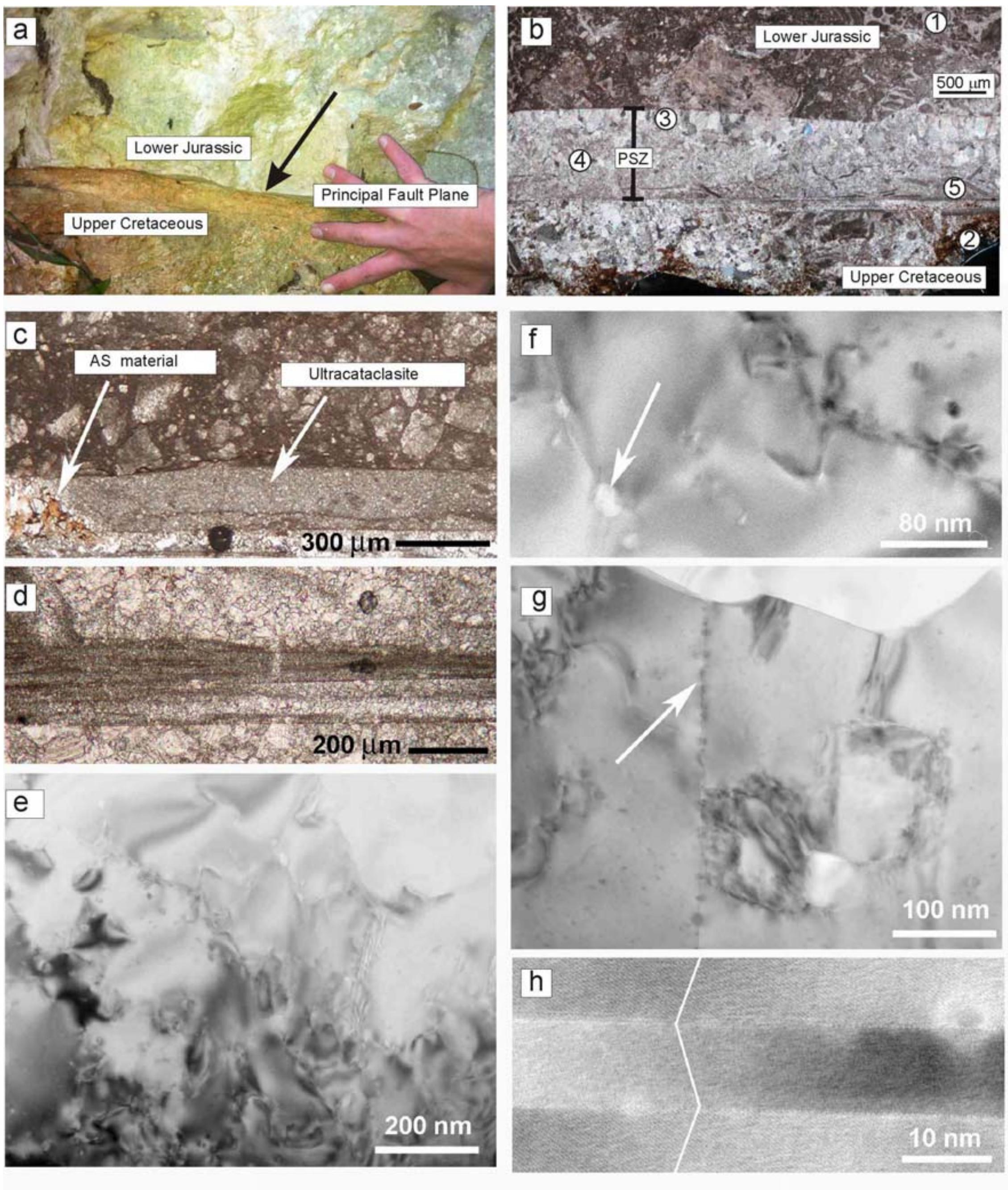

Figure DR1: a) Details of the Principal Fault Plane at the outcrop scale: arrow indicates the contact imaged in b. Micro/nanostructures of the Principal Slip Zone in optical microscope, crossed nicols (b) and parallel nicols (c, d) and bright-field TEM (e, f, g, h) images.

The Spoleto thrust (Barchi and Brozzetti, 1991) brings the lower Jurassic massive carbonates of the Calcare Massiccio formation onto upper Cretaceous layered carbonates, with clay-rich intercalations of the Scaglia Rossa formation (Alvarez et al., 1978). The fault contact is represented by a distinct principal fault plane (Fig. DR1a) that can be followed with continuity for more than 50 m. At the microscale (Fig. DR1b) the principal fault plane consists of a Principal Slip Zone, PSZ, that separates a 0-20 cm thick cataclasite formed at the expense of lower Jurassic Calcare Massiccio carbonates in the hanging wall, from a > 20 m thick cataclasite formed from the upper Cretaceous carbonates of the Scaglia Rossa. In the hanging wall cataclasite, the typical sedimentary texture of the Calcare Massiccio with ooid grains (Fig. DR1b point 1) is preserved in some large grains of the fault rock. In the footwall block the fault rock is made of carbonates and illite-smectite (the brown material around point 2 in Fig. 2b). In some portions, the PSZ is represented by a sharp layer, ~ 1 mm thick, with one boundary characterized by blocky calcite (Fig. DR1b point 3). The calcite fibres oriented with their long axes vertical, indicate that the pore pressure must have exceeded the lithostatic stress when hydrofracturing occurred. Along the PSZ, remnants of calcite veins are dispersed within the ultracataclasite (Fig. DR1b, point 4). Some portions of the PSZ are characterized by a closely packed, micrometer-sized (0.1-10 μm) ultracataclasite (Fig. DR1c) that vanishes within the AS material. Segmented and discontinuous layers of the micrometer-sized ultracataclasite are present in other portions the PSZ (Fig. DR1b, point 5). Other structural features of the PSZ are represented by thin subparallel horizons of closely packed, micrometer-sized ultracataclasite (Fig. DR1d). The occurrence of re-worked closely packed ultracataclasite (Fig. DR1b, point 5) and calcite veins (Fig. DR1b, point 4) within the PSZ suggests a cyclic evolution of localization and grain size reduction plus fluid overpressure build up and veining during faulting. SEM and TEM investigations reveal that the ultracataclasite material consists exclusively of fine and ultrafine calcite grains, without clays or amorphous coatings (e.g. Schleicher et al., 2010). Calcite crystals show dislocations, subgrain boundaries (Fig DR1e), bubbles alignment along grain boundaries (arrow in Fig. DR1f) and twinning (arrow in Fig. DR1g and high magnification detail in Fig. DR1h).

**REFERENCE**

Barchi, M.R., and Brozzetti, F., 1991, Il Sovrascorrimento di Spoleto: un esempio di tettonica di inversione nell'Appennino Umbro-Marchigiano? Studi Geologici Camerti, v. 1, p. 337-345.
Schleicher, A.M., van der Pluijm, B.A., and Warr, L.N., 2010, Nanocoatings of clay and creep of the San Andreas fault at Parkfield, California: Geology, v. 7, p. 667–670.

**Data Repository Item DR2**: Mineralogical characterization of the cataclasite and ultracataclasite layer.

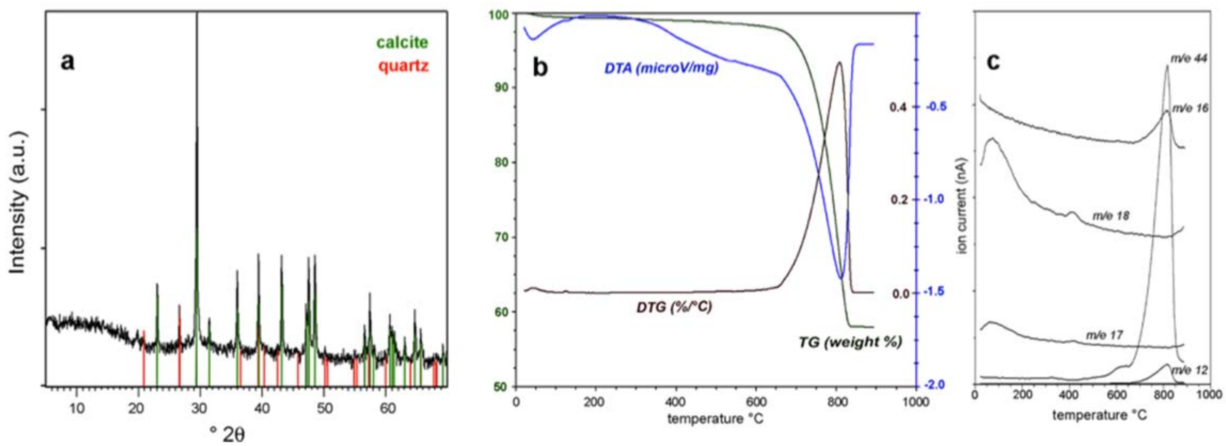


Figure DR2: XRPD (a), thermal analyses (b) and EGA spectra (c) for the cataclasite.

Conventional X-ray powder diffraction pattern (Fig. DR2a, Intensity, arbitrary units a.u., vs. diffraction angle, °2θ) of cataclasite reveals calcite and minor quartz as the main crystalline phases. Minor, poorly crystalline clays produce the broad and very weak signal at low diffraction angles.

Cataclasite has been also analyzed by thermogravimetry (TG, weight %, heating step of 10°/min), differential thermogravimetry (DTG, %/°C) and differential thermal analysis (DTA, μA/mg, endothermic signals down), coupled with emitted gas analysis, EGA, mass spectrometry (Figs. 1b and c). In EGA spectra (Fig. DR2c), m/e 17, 18 and m/e 12, 16, 44 peaks indicate dehydration and decarbonation reactions, respectively. Coupling DTA curve and EGA data, the weak endothermic signal at ~95 °C (Fig. DR2b) is attributed to adsorbed water loss in clays, followed by a broad endothermic signal starting at 400 °C, due to hydroxyl loss (EGA peak at ~415 °C). The overall weight loss before calcite decarbonation (i.e., up to 600 °C) is only 2%, confirming that clays are present in a low amount. Calcite decarbonation starts at ~600 °C and produces the main DTA signal at 800-820 °C (Fig. DR2b). Decarbonation produces a total weight loss of ~40 %, indicating ~92 wt.% calcite content in the cataclasite. The remaining 8% is illite-smectite and quartz.

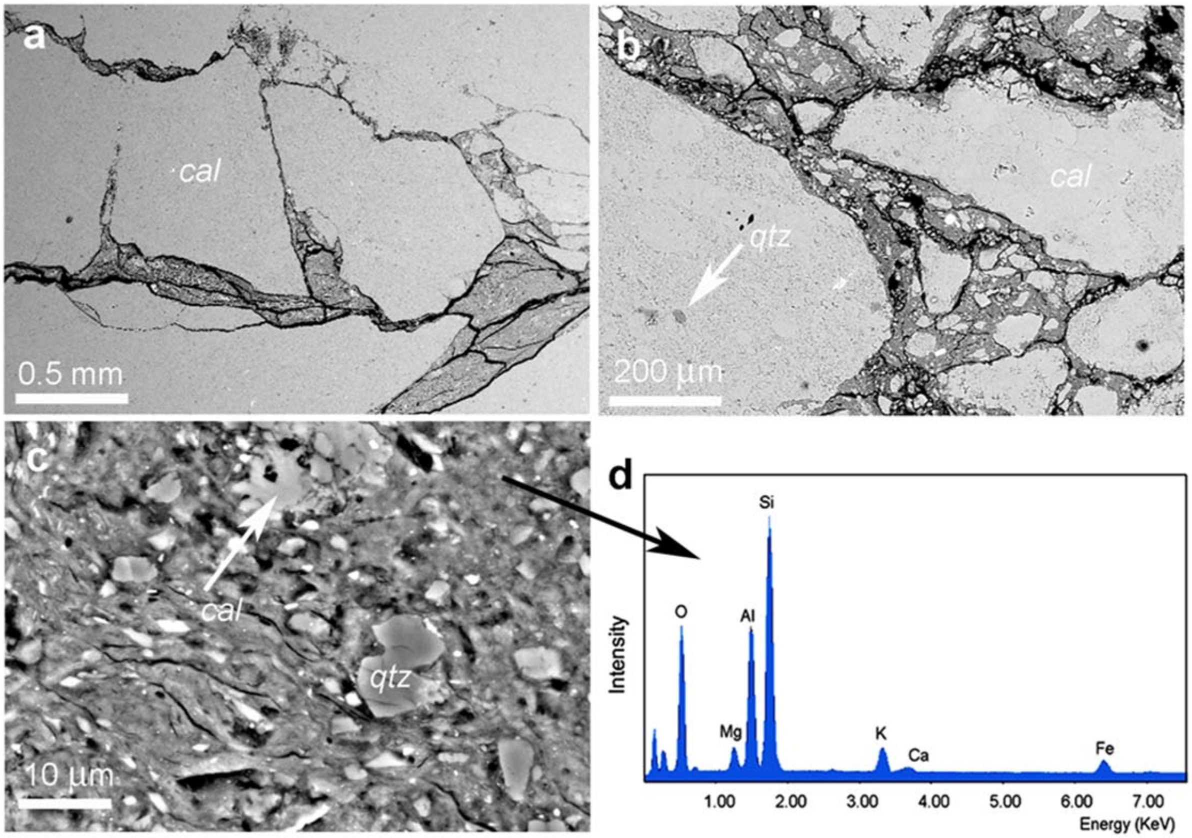


Figure DR3: BSE/SEM images (a, b, c) of cataclasite microstructure. The EDS spectrum (d) shows the composition of the ultrafine clay-rich material within pressure solution seams.

The footwall block cataclasite, derived from the upper Cretaceous Scaglia Rossa formation, consists of large clasts of microgranular calcite and rare quartz (Fig. DR3a), separated by pressure-solution seams, up to 0.5 mm wide (dark grey). Sharp-edge clasts are frequently embedded within the stylolitic material (Fig. DR3b). Pressure solution seams consist of a poorly crystalline fine-ultrafine material, including calcite relicts and different insoluble minerals (e.g., quartz, apatite, Fe-oxides, muscovite and chlorite; Fig. DR3c). The composition of the poorly crystalline material is consistent with illite-smectite clays (representative EDS spectrum in Fig. DR3d), as also confirmed by TEM investigations (unpublished data).